Latin American Journal of Solids and Structures
www.lajss.org

Superposition of Stress Fields in Diametrically Compressed Cylinders

Abstract

The theoretical analysis for the Brazilian test is a classical plane stress problem of elasticity theory, where a vertical force is applied to a horizontal plane, the boundary of a semi-infinite medium. Hypothesizing a normal radial stress field, the results of that model are correct. Nevertheless, the superposition of three stress fields, with two being based on prior results and the third based on a hydrostatic stress field, is incorrect. Indeed, this work shows that the Cauchy vectors (tractions) are non-vanishing in the parallel planes in which the two opposing vertical forces are applied. The aim of this work is to detail the process used in the construction of the theoretical model for the three stress fields used, with the objective being to demonstrate the inconsistency often stated in the literature.

Keywords

Brazilian Test, Elasticity Theory, Plane Stress, FEM Simulation.

João Augusto de Lima Rocha [a]
Alexandre de Macêdo Wahrhaftig [b]

[a,b] Federal University of Bahia (UFBa) Polytechnic School, Department of Construction and Structures, Rua Aristides Novís, 02, 5º andar, Federação, Salvador – BA, Brazil, CEP: 40210-910
[a] jrjoaroch@gmail.com
[b] alixa@ufba.br

http://dx.doi.org/10.1590/1679-78252674

Received 02.12.2015
In revised form 25.04.2016
Accepted 06.05.2016
Available online 18.05.2016

1 INTRODUCTION

The stress tensor for an elastic, diametrically compressed cylinder, as obtained by Timoshenko and Goodier (1970), is a result of technical interest because it is used as a basis in obtaining tension limits in fragile materials. With this purpose in mind, the artifice involving the superposition of three stress fields is used, selected specifically to ensure vanishing of the Cauchy vectors (*tractions*) on the surface of a cylindrical body immersed in a strip of infinite length. This procedure enables the cylindrical modelling of the well-known *Brazilian test*.

The main objective of this paper is to discuss the result obtained by Timoshenko and Goodier (1970) that Carneiro (1943-1947) used to determine the tension strength of brittle materials. The second objective is to verify whether the mistake in reasoning for the diametric compression test, conceived in 1943 for determination of the tension strength of concrete, prevents the use of the *Brazilian test*.

The intention of Carneiro (1943-1947) when constructing the theoretical model was to ensure that the *tractions* on the surface of a cylinder vanish when immersed in an endless flat strip of finite width with two opposing compressive forces applied vertically. The model used to remove the cylinder from the middle leads to an expression for the component (tension) in the vertical diametric plane of the cylinder, giving its dependence on the applied compressive load and the diameter of the cylinder. However, this result cannot be obtained because it is mischaracterized when introduced into the correct boundary conditions on the infinite faces for the upper and lower boundaries. Hence, the validity of the distribution of tension stresses is lost in the vertical diameter in analyzing the *Brazilian test*.

A careful literature review on the subject has revealed a wide range of scientific papers addressing different aspects of determining the limit stress of tension of materials, particularly brittle materials, by using the Brazilian test. Li and Wong (2013) show the evolution of the state of art about the subject, analysing the 43 most important works, in the view of the authors, from 1943–2011. The papers most directly related to this article are: Sheep (1943), Hondros (1959), Colback (1966), Jaeger and Hoskins (1966), Jaeger (1967), Hudson et al. (1972), Wijk (1978), Yanagidani et al. (1978), Sundaram and Corrales (1980), Yu et al. (2006) and Markides et al. (2010, 2011). These publications were critically examined, but did not reveal any references to the aspects emphasised here. It is also worth mentioning the contributions of Lanaro et al. (2009), Andreev (1991), Markides et al. (2012), Erarslan et al. (2012) and Aydin and Basu (2006), Yang et al (2015), Haeri et al (2014), Choupania et al (2015), Cai et al (2015), which addressed the issue of the Brazilian test, either theoretically or experimentally, or even applied. However, none of them investigated the foundations raised from Timoshenko and Goodier (1970), in which the problem of methodological character examined in this work was found.

The discussion presented below questions the determination of the tension strength used in the diametrical compression test but does not enable one to immediately conclude fault in the *Brazilian test*. What one finds in discussing this issue is that there is no exact solution to the problem, as previously supposed. For this reason, we performed a numerical experiment with FEM to obtain the tension stress profile at the diametric vertical plane of a cylinder compressed diametrically. Numerical experimentation indicates the occurrence of a value for the tension stress in the center of the cylinder, which is roughly equivalent to the maximum and was used by Carneiro for all points along the vertical diametrical plane. This confirmation can only now be made because the computational modelling capabilities were not previously available.

2 THEORETICAL BASIS OF THE ELASTIC MODEL OF THE *BRAZILIAN TEST*

The analysis of the stress distribution within a cylinder subjected to two lines of symmetrical longitudinal loads acting along a pair of opposing generatrices of a cylinder can be found in the work of Timoshenko and Goodier (1970). The article used here as reference is the English version published in 1970. The basis of this analysis is the classical stress distribution for a semi-infinite plate of uniform thickness in a plane stress state (see Figure 1 and Figure 2), as motivated by Timoshenko and Goodier (1970). We emphasize that we do not discuss the solution of the problem with a load applied to the upper plane of a semi-infinite medium, but rather the superposition of stresses that forms the basis of this result.

2.1 Stress Field Resulting from the Application of a Concentrated Normal Load to the Plane Limit of a Semi-Infinite Elastic Middle

According to Timoshenko and Goodier (1970), there is a basic solution in the theory of elasticity called the *simple radial distribution* that satisfies the equilibrium equations of the bi-dimensional problem. As shown in Figure 1, the domain of the problem reduces to an arbitrary cross-section of the cylinder, as indicated, where the body forces per unit volume, R and S, are considered null. The equations for the general local equilibrium in the polar representation are:

$$\begin{aligned} &\frac{\partial \sigma_r}{\partial r} + \frac{1}{r}\frac{\partial \tau_{r\theta}}{\partial r} + \frac{\sigma_r - \sigma_\theta}{r} + R = 0 \\ &\frac{1}{r}\frac{\partial \sigma_\theta}{\partial \theta} + \frac{\partial \tau_{r\theta}}{\partial r} + \frac{2\tau_{r\theta}}{r} + S = 0. \end{aligned} \tag{1}$$

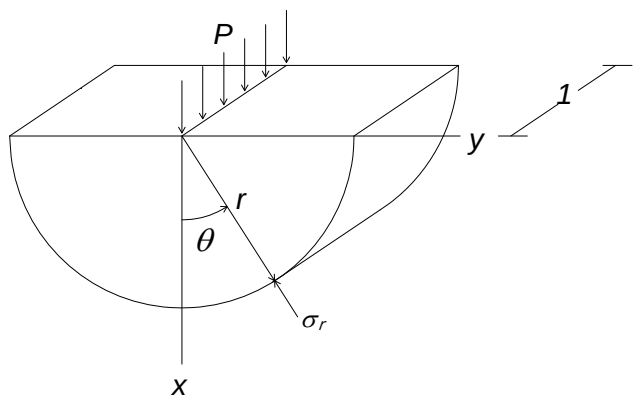

Figure 1: Radial stress field due to a uniformly distributed load P.

In terms of the stress function $\varphi = \varphi(r, \theta)$, the tensor components that satisfy Eq.(1) for null R and S are given by:

$$\begin{aligned} \sigma_r &= \frac{1}{r}\frac{\partial \varphi}{\partial r} + \frac{1}{r^2}\frac{\partial^2 \varphi}{\partial \theta^2} \\ \sigma_\theta &= \frac{\partial^2 \varphi}{\partial r^2} \\ \tau_{r\theta} &= \frac{1}{r^2}\frac{\partial \varphi}{\partial \theta} - \frac{1}{r}\frac{\partial^2 \varphi}{\partial r \partial \theta} = -\frac{\partial}{\partial r}\left(\frac{1}{r}\frac{\partial \varphi}{\partial \theta}\right). \end{aligned} \tag{2}$$

A function $\varphi = \varphi(r, \theta)$ must be found that solves the unique compatibility equation for the plane problem, i.e.

$$\left(\frac{\partial^2}{\partial r^2} + \frac{1}{r}\frac{\partial}{\partial r} + \frac{1}{r^2}\frac{\partial^2}{\partial \theta^2}\right)\left(\frac{\partial^2 \varphi}{\partial r^2} + \frac{1}{r}\frac{\partial \varphi}{\partial r} + \frac{1}{r^2}\frac{\partial^2 \varphi}{\partial \theta^2}\right) = 0. \tag{3}$$

For the simple radial distribution, the stress function satisfying Eq. (3) is:

$$\varphi = -\frac{P}{\pi} r\theta \sin\theta$$

Substituting this function into Eq. (2) yields:

$$\begin{aligned} \sigma_r &= \frac{1}{r}\frac{\partial\varphi}{\partial r} + \frac{1}{r^2}\frac{\partial^2\varphi}{\partial\theta^2} = -\frac{2P}{\pi}\frac{\cos\theta}{r}, \\ \sigma_\theta &= \frac{\partial^2\varphi}{\partial r^2} = 0, \\ \tau_{r\theta} &= -\frac{\partial}{\partial r}\left(\frac{1}{r}\frac{\partial\varphi}{\partial\theta}\right) = 0. \end{aligned} \tag{4}$$

The first equation of Eq. (4) implies that the resultant forces acting on the cylindrical surface of radius r (Figure 1) and uniform thickness balance load P, i.e.:

$$2\int_0^{\pi/2} \sigma_r r\cos\theta\, d\theta = -\frac{4P}{\pi}\int_0^{\pi/2} \cos^2\theta\, d\theta = -P. \tag{5}$$

With respect to the boundary conditions, one obtains from Eq. (4) $\sigma_r = \sigma_\theta = \tau_\theta = 0$ in the upper part (Figure 1) of the flat plate representative of the problem, i.e., on the length AB for which $\cos\theta = 0$, excepting the point O where load $P(r = 0)$ is applied. The load is actually a distribution over an area near the load application point, which necessarily falls within the plastic accommodation regimen. Hence, the equations of linear elasticity are valid only outside this restricted area.

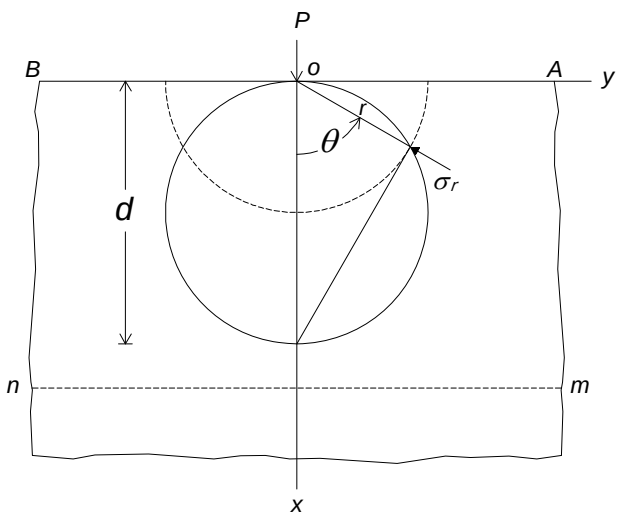

Figure 2: Stress field (state plane) for points on the circumference of the circle tangent to O.

When verifying the compatibility of the stress distribution represented by Eq. (4) with the distribution of the *tractions* over the remaining contour beyond the flat outer surface represented by

AB in Figure 2, we take the region $ABmn$ to extend to infinity and the value of r also to tend to infinity. Hence, the stresses must vanish:

$$r \to \infty \Rightarrow \sigma_r, \sigma_\theta \text{ and } \tau_\theta \to 0. \tag{6}$$

For a generic point on the circumference of the circle with diameter d tangent to point O, the point where the load is applied (Figure 2), it follows that:

$$r = d\cos\theta, \tag{7}$$

where d is the diameter of the circle. Thus, if Eq. (7) is substituted into the first of Eq. (4), one obtains:

$$\sigma_r = -\frac{2P}{\pi d}. \tag{8}$$

This result indicates that at every point (except O) on the circle's circumference, a load P applied to point O leads to a stress component (compression) in the radial direction (dashed circle in Figure 2) of a magnitude that conforms to Eq. (8).

2.2 Stresses in a Circular Disc with Two Diametrically Opposite Vertical Loads

Following Timoshenko and Goodier (1970), our theoretical development makes use of results given in the previous section for the construction of a stress field composed as a superposition of two symmetrical fields: the first generated by the application of force P at point A, and the second by the application of the force P in the opposite direction at point B (see Figure 3).

The first stress field has its source in the semi-infinite domain bounded above by the tangent plane at point A; the second field has as its domain the semi-infinite region bounded below by the tangent plane at point B. The region of intersection, where the superposition of the two fields is given, is located in a range of finite width and infinite length, situated between the two horizontal planes. It is therefore a composite model to be used with the possibility of isolating the cylindrical body under diametric compression from this elastic medium. Assuming that each field is the simple radial stress distribution given in the previous section, then, according to the first equation of Eq. (4), the normal components of the field tensor related to the force P applied at A are (see Figure 4):

$$\sigma_r = -\frac{2P}{\pi}\frac{\cos\theta}{r}. \tag{9}$$

By analogy, the normal component of the field corresponding to force P applied in the opposite direction at point B (Figure 4) is:

$$\sigma_r = -\frac{2P}{\pi}\frac{\cos\theta_1}{r_1}. \tag{10}$$

From the property of triangles inscribed in a semicircle, r and r_1 in Figure 4 are perpendicular to each other; hence,

$$\frac{\cos\theta}{r} = \frac{\cos\theta_1}{r_1} = \frac{1}{d}, \tag{11}$$

where d is the circular diameter section. Substituting Eq. (11) into Eqs. (9) and (10) leads to values given by Eq. (8) for the normal stress in both planes, allowing the conclusion that at the generic point M in Figure 5, the principal stresses are compressive, both with the same magnitude. This means that at any point on the cylinder indicated by the contour of the circumference there is a *hydrostatic plane* system of stresses such that, for all tangent planes through M, the Cauchy vectors have the same magnitude, each one normal to its respective plane and corresponding to the compressive forces.

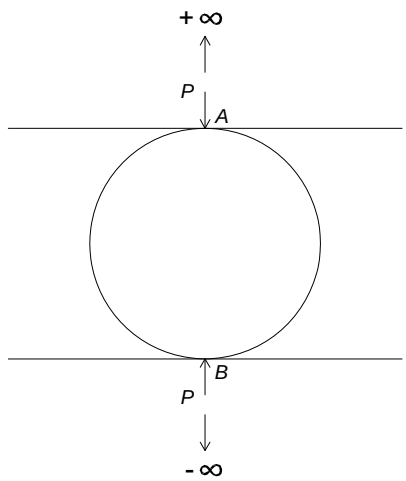

Figure 3: Superposition of two symmetrical stress fields for construction of the model of a cylinder compressed diametrically.

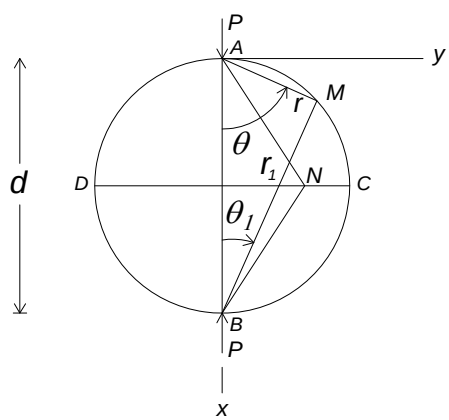

Figure 4: Application of two opposite loads with module P.

Figure 5 illustrates the fact that, in the neighborhood of any point M, the Cauchy vector must have the same magnitude in the two orthogonal planes for the element indicated and must be compressive with a value given by Eqs. (10) and (11):

$$\sigma = -\frac{2P}{\pi d}. \tag{12}$$

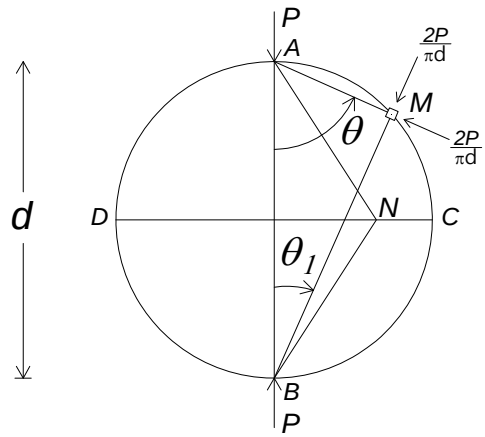

Figure 5:Principal stresses at a generic point M of the boundary of the circle.

2.3 Obtaining the Third Stress Field to Superimpose with the Previous Two

Following this reasoning, to simulate a disk compressed diametrically, superposing one more stress fields is required. Specifically, this field needs to make the sum of all *tractions* disappear in the contour of the cylindrical body located at the intersection of the semi-infinite spaces depicted in Figure 3. Observing **Figure 5**, it appears that at every point of the circumference, all of the principal stresses are equal to 2π/PD and of compression, obtained by the setting of a hydrostatic stress state. In order to annul the tensions in the circumference points, it is sufficient to superimpose a uniform field with a diagonal tensor that has the first two components of the same module, but of traction, as Eq. (13).

$$T = \begin{bmatrix} 2P \,/\, \pi d & 0 & 0 \\ 0 & 2P \,/\, \pi d & 0 \\ 0 & 0 & 0 \end{bmatrix}. \tag{13}$$

From the above results, the superposition is composed of three contributions:

a) the field produced by the load P applied at A in the semi-infinite domain below the tangent plane through A;

b) the field produced by the load P applied at B in the semi-infinite domain above the tangent plane through B; and

c) the field represented by the tensor that produces *tractions* in the contour of the circle that cancel the *tractions* resulting from the superposition of the two previous fields, throughout the infinite domain.

By analogy to 0, for which the components of the stress were obtained by Eq. (4), the stress field of b), described in polar coordinates (pole at point B) in accordance with the depiction in Figure 4, also has only a non-zero component in the radial direction, i.e.,:

$$\begin{aligned} \sigma_r &= -\frac{2P}{\pi}\frac{\cos\theta_1}{r_1}, \\ \sigma_\theta &= 0, \\ \tau_{r\theta} &= 0. \end{aligned} \tag{14}$$

Finally, apart from the two diametric compression forces P applied at A and B, one completes the model of the cylinder free from external forces on its exterior surface. The model enables the state of stress on the points of the cylinder to be represented in cross-sections more properly while in a plane stress state.

After forming the superposition of the fields given by Eqs. (4), (14), and (15), in the Cartesian system of Figure 4, for any point on the circle, the values of the stress components for the plane stress state are given by:

$$\begin{aligned} \sigma_x &= -\frac{2P}{\pi}\frac{\cos\theta}{r}\cos^2\theta - \frac{2P}{\pi}\frac{\cos\theta_1}{r_1}\cos^2\theta_1 + \frac{2P}{\pi d}, \\ \sigma_y &= -\frac{2P}{\pi}\frac{\cos\theta}{r}sin^2\theta - \frac{2P}{\pi}\frac{\cos\theta_1}{r_1}sin^2\theta_1 + \frac{2P}{\pi d}, \text{ and} \\ \tau_{xy} &= -\frac{2P}{\pi}\frac{\cos\theta}{r}sin\theta\cos\theta + \frac{2P}{\pi}\frac{\cos\theta_1}{r_1}sin\theta_1\cos\theta_1. \end{aligned} \tag{15}$$

By virtue of Eq. (11), at any point on the circumference of the circle $ACBDA$ in Figure 5, Eq. (15) leads to:

$$\sigma_x = \sigma_y = \tau_{xy} = 0. \tag{16}$$

Although it is necessary to isolate the cylinder from the infinite medium, the vanishing of the *tractions* at any point on the circumference of the cylinder section is not sufficient. The result needs to be consistent with the boundary conditions in the tangent planes passing through loading points A and B (see Figure 6).

3 DISCUSSION OF THE RESULTS FROM THE CURRENT MODEL SIMULATING DIAMETRICAL COMPRESSION

Using Eq. (15), which is assumed true, we calculated the *tractions* in the tangent planes through A and B, according to the scheme shown in Figure 6.

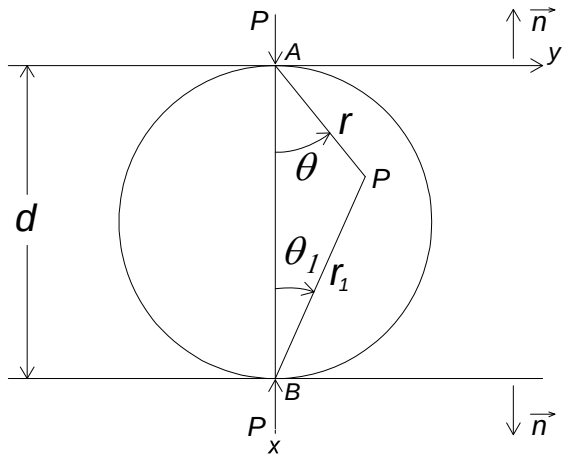

Figure 6: Superposition of two valid fields on semi-infinite domains.

For points in the plane through A, recall that

$$\theta = \frac{\pi}{2} \text{ and } r_1 = \frac{d}{\cos\theta_1}\,. \tag{17}$$

Aided by Eq. (15), one then obtains the stresses tensor components:

$$\begin{aligned} \sigma_x &= \frac{2P}{\pi\, d}\sin^2\theta_1, \\ \sigma_y &= \frac{2P}{\pi\, d}\cos^2\theta_1, \text{ and} \\ \tau_{xy} &= \frac{2P}{\pi\, d}\sin\theta_1\cos\theta_1. \end{aligned} \tag{18}$$

With the unit normal vector in this plane defined as

$$\mathbf{n} = (-1;0;0), \tag{19}$$

the *tractions*, based on Eqs. (15) and (19), are:

$$\mathbf{t} = (-\frac{2P}{\pi\, d}sin^2\theta_1; -\frac{2P}{\pi\, d}sin\theta_1\cos\theta_1; 0). \tag{20}$$

Similarly, for the tangent plane through point B, the external unit normal vector is:

$$\mathbf{n}_1 = (1;0;0), \tag{21}$$

with

$$\theta_1 = \frac{\pi}{2} \text{ and } r = \frac{d}{\cos\theta}\,, \tag{22}$$

the values of the non-zero stress components of the tensor, according to Eqs. (15) and (22), are

$$\begin{aligned} \sigma_x &= \frac{2P}{\pi d} sin^2\theta, \\ \sigma_y &= \frac{2P}{\pi d} \cos^2\theta\ , \\ \tau_{xy} &= \frac{2P}{\pi d} sin\theta\cos\theta. \end{aligned} \tag{23}$$

So, the *tractions* in this plane are expressed as

$$\mathbf{t}_1 = (\frac{2P}{\pi d} sin^2\theta; \frac{2P}{\pi d} sin\theta\cos\theta; 0). \tag{24}$$

Eqs. (20) and (24) show that the boundary conditions are not identically zero on the tangent planes through A and B (apart from these two points), as is desired if the values of the stresses in the cylinder with a boundary free of *tractions* were correct.

To illustrate, Figure 7 shows graphically the distribution of the normal components of the *tractions* over both the upper and lower tangent planes, given by Eqs. (20) and (24), respectively. Evidently, the values of the stress components given by Eq. (15) do not guarantee that both components of the *tractions* are zero in those planes. Hence, they must be rejected in applying the diametrical compression model used in the *Brazilian test*.

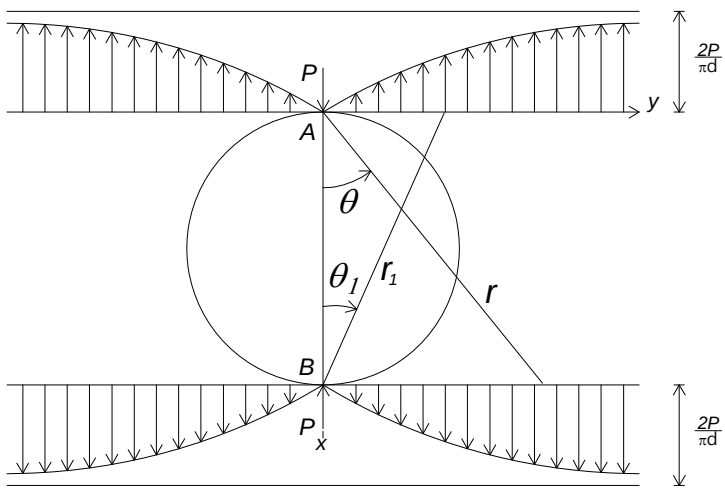

Figure 7: Distribution of the normal component for *tractions* in the tangent planes through A and B.

4 COMPUTATIONAL MODELLING

The numerical computational modelling was performed using the finite element method (FEM) with elements in the plane stress state, according to SAP2000 (integrated software for structural analysis and design, Analysis Reference Manual, Computer and Structures, Inc., Berkeley, Califor-

nia, USA, 2015), a commercial software package. The loading conditions used in computer simulation were meant to represent the procedures stated in conducting the Brazilian test, as represented in **Figure 3**. For that, both identical and opposing forces were applied, one positioned at the upper end and one at the bottom end of the cylinder. Care was taken to restrict it across, in one direction, to avoid any possibility of lateral instability, characterising then a plane stress state. Figure 8 exemplifies the output and discretisation using the computational modelling employed in a similar way for all the models. It is interesting to mention that the plane element is appropriated to model plane-stress behavior in two-dimensional solids where the stresses are assumed not to vary in the thickness direction. The element has no out-of-plane stiffness and because of this there is no stress acting perpendicularly to element, existing, therefore, the transversal deformation at the plane which contents it, or better, the plane-stress element contributes stiffness only to the degrees of freedom in the plane of the element. For more details on the FEM, the reader is referred to Bucalem and Bathe (2011) and Cook (1974).

The distribution of the normal stresses in the tangent plane element can be observed in Figure 9, where the radius is partitioned into nine bins with 1 indicating the central point of the circle and 9 indicating its surface. The previous results were developed for a cylinder of 10 cm diameter subject to opposing forces of 40.000 N, which could have any other value, applied vertically on the circumference. The equation currently recommended for the *Brazilian test*, i.e., σ_y, in Eq. (12), provides a maximum tension stress of 254647.91 Pa, whereas that obtained in the computational modelling was 254335.45 Pa, 99.88% of the previous. Other computational experiments using the same FEM as above were performed. From 12 tests with diameters between 10 cm and 200 cm, similar behaviors were observed in regard to the distribution of the normal stress component perpendicular to the vertical diameter of the cylinder.

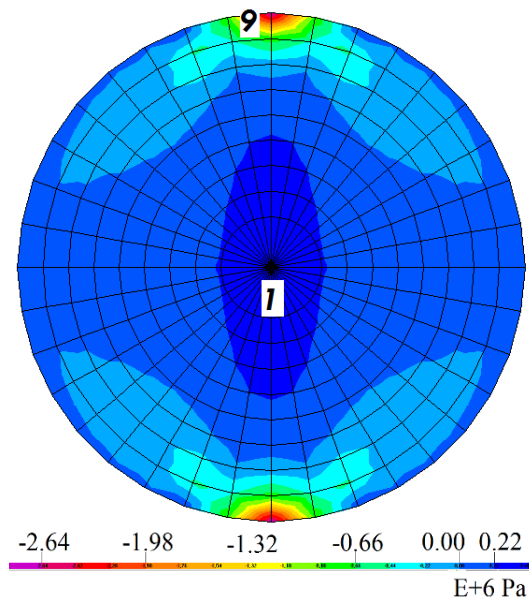

Figure 8: Polar diagram of the horizontal normal components using FEM.

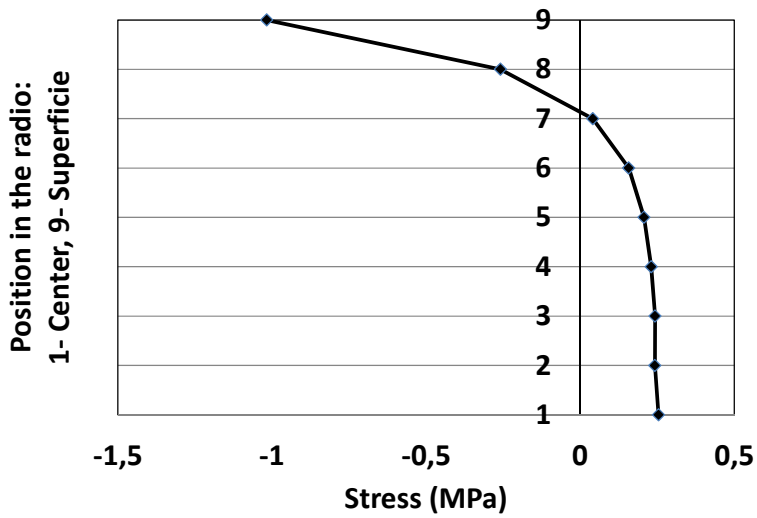

Figure 9: Distribution of the normal components by FEM.

5 CONCLUSIONS

Given the present discussion and considering the results obtained, we determined that contrary to statements in the literature, there is no exact mathematical expression for the component of normal stress (tension) along points in the vertical diametrical plane of a cylinder used in diametrical compression tests. This finding implies that the mathematical expression employed in the work of Carneiro (1947) is methodologically incorrect because it relates this component of stress to the vertical force applied and the diameter of the cylinder used in the *Brazilian test*.

This error arises because the superposition of three stress fields, introduced to obtain a solution to the elastic problem, yields vanishing tractions on the surface of the cylinder immersed in an infinite medium, but does not preserve the boundary conditions in the tangential planes that form the upper and lower boundaries of the domain in which the cylinder is immersed. The tractions in those planes also need to vanish everywhere except for the points of application of the loads to the cylinder. This is the key point of the present discussion, because it is not considered in the classical model presented by Timoshenko (1970).

The misconception that exists in taking the superposition of the three fields of tension stems from a mistake perpetrated in a previous application of the results to the construction of a theoretical model for diametrical compression tests established independently by Carneiro (1943-1947) and Akasawa (1943). Fortunately, as evidenced by our numerical experiments using FEM, the maximum diametrical tension stress in the center of the cylinder tends to $2P/\pi d$, a value that has been traditionally and mistakenly accepted as valid for all points in the vertical diametrical plane of the cylinder. Strictly speaking, this value for tension stress only occurs at the center of the cylinder, implying that rupturing in the sample in the *Brazilian test* originates from the center.

References

Akazawa, T. (Nov., 1943). Méthode pour l'essai de traction de bétons, Journal of the Japanese Civil Engineering republished, in French, by Bulletin RILEM 16, Paris (Nov. 1953), p. 11–23.

Andreev, G.E. (1991). A review of the Brazilian test for rock tensile strength determination. Part I: calculation formula. *Mining Science and Technology,* 13, 445-456.

Aydin, A. and Basu, A. (2006). Technical Note The use of Brazilian Test as a Quantitative Measure of Rock Weathering. Rock Mech. Rock Engng. (2006) 39 (1), 77–85. doi:10.1007/s00603-005-0069-0.

Bucalem, M.L., Bathe, K.J. (2011). The Mechanics of Solids and Structures – Hierarchical Modelling and the Finite Element Solution, Springer, Heidelberg.

Cai, Y., Yu, S., Lu, Y. (2015). Experimental study on granite and the determination of its true strain-rate effect, Lat. Am. j. solids struct.12, 4, 675-694, doi:10.1590/1679-78251331.

Carneiro, F.L.L.B. (1943). A new method for determining the tension stress in the concrete. Proceedings of 5th Meet of Association Brazilian for Standardization - ABNT, 3th Section, Sept, 16, p.126–129 (in Portuguese).

Carneiro, F.L.L.B. (Jun., 1947). Résistance à la traction des bétons – Une nouvelle méthode pour La détermination de La résistance à la traction des bétons, presented to the International Meeting of Testing Laboratories, founding of RILEM.

Choupania, M., Ayatollahia, M.R., Mallakzadeh, M. (2015). Investigation of Fracture in an Interface Crack Between Bone Cement and Stainless Steel. Lat. Am. j. solids struct., 12, 3, 446-460, doi:10.1590/1679-78251142.

Colback, P.S.B. (1966). An analysis of brittle fracture initiation and propagation in the Brazilian test. In: Paper presented at the Proceedings of the First Congress International Society of Rock Mechanics, Lisbon, Portugal.

Cook, R.D. (1974). Concepts and Applications of Finite Element Analysis. John Wiley and Sons, Inc., New Jersey.

Erarslan, N., Liang, Z. Z., Williams, D. J. (2012). Experimental and Numerical Studies on Determination of Indirect Tensile Strength of Rocks. Rock Mech Rock Eng (2012) 45:739–751. doi:10.1007/s00603-011-0205-y.

Haeri, H., Shahriar, K., Marji, M.F., Moarefvand, P. (2014), On the crack propagation analysis of rock like Brazilian disc specimens containing cracks under compressive line loading. Lat. Am. j. solids struct. 11, 8, 1400-1416. doi: 10.1590/S1679-78252014000800007.

Hondros, G. (1959). The evaluation of Poisson's ratio and the modulus of materials of a low tensile resistance by the Brazilian (indirect tensile) test with particular reference to concrete. Aust J Appl Sci 10(3):243–268.

Hooper, J. A. (1970). The Failure of Glass Cylinders in Diametral Compression. J. Mech.P hys.S olids, 1971, Vol. 19, pp. 179 to 200.

Hudson, J.A., Brown, E.T., Rummel, F. (1972) The controlled failure of rock discs and rings loaded in diametral compression. Int J Rock Mech Min Sci Geomech Abstr 9(2):241–248. doi:10.1016/0148-9062(72)90025-3.

Jaeger, J.C. (1967). Failure of rocks under tensile conditions. Int J Rock Mech Min Sci Geomech Abstr 4(2):219–227. doi:10.1016/0148-9062(67)90046-0.

Jaeger, J.C., Hoskins, E.R. (1966). Rock failure under confined Brazilian test. J Geophys Res 71(10):2651–2659.

Lanaro, F., Sato, T., Stephansson, O. (2009). Microcrack modelling of Brazilian tensile tests with the boundary element method, International Journal of Rock Mechanics & Mining Sciences 46 (2009) 450–461. doi:10.1016/j.ijrmms.2008.11.007.

Markides, C.F., Pazis, D.N, Kourkoulis, S.K. (2012) The Brazilian disc under non-uniform distribution of radial pressure and friction. Int J Rock Mech Min Sci 50(1):47–55. doi:10.1016/j.ijrmms.2011.12.012.

Markides, C.F., Pazis, D.N., Kourkoulis, S.K. (2010). Closed full-field solutions for stresses and displacements in the Brazilian disk under distributed radial load. Int J Rock Mech Min Sci 47(2):227–237. doi:10.1016/j.ijrmms.2009.11.006.

Markides, C.F., Pazis, D.N., Kourkoulis, S.K. (2011). Influence of friction on the stress field of the Brazilian tensile test. Rock Mech Rock Eng 44(1):113–119. doi:10.1007/s00603-010-0115-4.

SAP 2000: Integrated software for structural analysis and design, Analysis Reference Manual, Computer and Structures, Inc. Berkeley, California, USA (2015).

Sundaram, P.N., Corrales, J.M. (1980). Brazilian tensile strength of rocks with different elastic properties in tension and compression. Int J Rock Mech Min Sci Geomech Abstr 17(2):131–133. doi:10.1016/0148-9062(80)90265-x.

Timoshenko, S.P., Goodier J.N. (1970). Theory of Elasticity, 3rd edition, McGraw-Hill.

Wijk, G. (1978). Some new theoretical aspects of indirect measurements of the tensile strength of rocks. Int J Rock Mech Min Sci Geomech Abstr 15(4):149–160. doi:10.1016/0148-9062(78)91221-4.

Yanagidani, T., Sano, O., Terada, M., Ito, I. (1978). The observation of cracks propagating in diametrically-compressed rock discs. Int J Rock Mech Min Sci Geomech Abstr 15(5):225–235. doi:10.1016/0148-9062(78)90955-5.

Yang, Fe., Ma, H., Jing, L., Zhao, L., Wang, Z. (2015). Dynamic compressive and splitting tensile tests on mortar using split Hopkinson pressure bar technique, Lat. Am. j. solids struct. 12, 4. 730-746. doi:10.1590/1679-78251513.

Yu Y., Yin J., Zhong Z. (2006) Shape effects in the Brazilian tensile strength test and a 3D FEM correction. Int J Rock Mech Min Sci 43(4):623–627. doi:10.1016/j.ijrmms.2005.09.005.